Communications in Physics, Vol. 32, No. 1 (2022), pp. 11-20
DOI: https://doi.org/10.15625/0868-3166/16014

HIGHLY-SENSITIVE REFRACTOMETER BASED ON A D-SHAPED FIBER BRAGG GRATING INTEGRATED INTO A LOOP-MIRROR OPTICAL FIBER LASER

PHAM THANH BINH[1,2,†], NGUYEN THUY VAN[1], PHAM VAN HOI[1,2], BUI HUY[1,2], HOANG THI HONG CAM[3], DO THUY CHI[4] and NGUYEN ANH TUAN[4]

[1]*Institute of Materials Science, Vietnam Academy of Science and Technology, 18 Hoang Quoc Viet, Cau Giay, Hanoi, Vietnam*

[2]*Graduate University of Science and Technology, Vietnam Academy of Science and Technology, 18 Hoang Quoc Viet, Cau Giay, Hanoi, Viet Nam*

[3]*University of Science and Technology of Hanoi, Vietnam Academy of Science and Technology, 18 Hoang Quoc Viet, Cau Giay, Hanoi, Viet Nam*

[4]*Thai Nguyen University of Education, 20 Luong Ngoc Quyen, Thai Nguyen, Viet Nam*

E-mail: †binhpt@ims.vast.ac.vn

Received 15 April 2021; *Accepted for publication 26 May 2021*; *Published 15 January 2022*

Abstract. *We report a new type of refractometer based on a D-shaped fiber Bragg grating (FBG) integrated in a loop-mirror optical fiber laser. This proposed sensor is used in wavelength interrogation method, in which the D-shaped FBG is applied as a refractive index (RI) sensing probe and a mirror to select mode of laser. The sensor is run by monitoring the wavelength shift of selected laser mode. The D-shaped FBG is prepared by the removal of a portion of the fiber cladding covering the FBG by means of side-polishing technique. The D-shaped FBG sensing probe integrated in a loop-mirror optical fiber laser with saturated pump technique for improving the sensing signals including more stable intensity, narrower bandwidth and higher optical signal-to-noise ratio compared to normal reflection configuration. The limit of detection (LOD) of this sensor can be achieved to 2.95 x 10-4 RIU in the refractive index (RI) range of 1.42-1.44. Accordingly, we believe that the proposed refractometer has a huge potential for applications in biochemical-sensing technique.*

Keywords: D-shaped FBG; optical fiber refractometer; loop-mirror optical fiber laser.

Classification numbers: 42.60.Da; 42.81.Gs; 42.79.Dj.

I. INTRODUCTION

Environmental pollutions are among great challenges in the human society with many pollutants, such as pesticides, nitrites, heavy metals, herbicides, antibiotics and other additives. Normally, pollutants are detected by various laboratory based techniques, such as chromatography, mass spectrometry, X-ray fluorescence spectrum, atomic fluorescence spectrometry, etc. [1–4]. These techniques are high sensitivity and accuracy instruments but very expensive and require professional to treat samples and operate instruments in centralized laboratories. Hence, it is essential to investigate new generation sensors, such as colorimetric, electrochemical, acoustic, field-effect transistor (FET) devices, surface-enhanced Raman scattering (SERS) and optical fiber sensors [5–11]. Among those, the optical fiber sensors have been rapidly developed because of their distinct advantages such as low signal attenuation, compact size, small sample volume, high flexibility, immunity from interference of electromagnetic fields, and remote sensing possibility [12, 13]. In recent years, optical fiber sensors for RI sensing have become one of the hot topics in optical sensing for chemical and biological sensing [14,15]. For various chemical and biochemical applications, RI sensing method is significant in which several substances can be detected by monitoring the effect of their refractive indices on the optical signals. The optical fiber RI sensors have attracted much attention and numerous optical fiber RI sensors have been reported, i.e., sensors based on surface plasmon resonance [16, 17], surface functionalized optical fiber [18, 19], etched-FBG [20, 21], photonic crystal fiber [22], long period fiber grating (LPG) [23], tilted fiber Bragg grating (TFBG) [24], tapered fiber [25], twin-core fiber [26], C-shaped fiber [27], D-shaped optical fiber with coated graphene-based indium tin oxide based on surface plasmon resonance effect [28], D-shaped fiber grating with using transmission configuration [29], D-shaped plastic optical fiber (POF) for an evanescent field absorption [30] in an attempt to improve the performances of RI sensors.

In this paper, we propose a novel optical fiber refractometer using a loop-mirror optical fiber laser structure integrated a D-shaped FBG as sensing probe which has a great advantage in sensing such as high intensity and narrow spectral line-width of the sensing signal response, and improved LOD. The proposed sensor is demodulated by wavelength shift. The lasing spectral response of the sensor is obtained at high intensity and kept stable by applying saturated pump technique. The D-shaped FBG functioned as a sensing probe is suitable for bio- and/or chemical sensors. The feasibility of the proposed sensor is investigated when the RI of the medium changes from 1.42 to 1.44 and the sensor exhibits a sensitivity and LOD of 33.94 nm/RIU and 2.95×10^{-4} RIU, respectively. These improved characteristics of this sensor make the proposed sensor promising for diverse applications, especially for the monitoring of chemical pollutants in aqueous environments.

II. EXPERIMENT

II.1. Preparation of D-shaped FBG sensing probe

In our study, D-shaped FBG sensing probe is prepared from the original FBG. Normally, the original FBG is known to be insensitive to the RI change of the surrounding environment since the fiber core is enfolded by a thick cladding.

The main principle of RI sensing is based on the interaction of the evanescent field with the measurement sample, which is proportional with the depth of the penetration of the evanescent

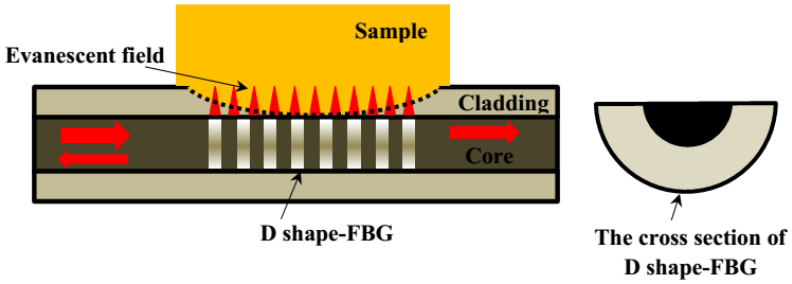

Fig. 1. Evanescent field in a D-shaped FBG sensing probe.

field (d_p), as given by Eq. (1) [31].

$$d_p = \frac{\lambda_0}{2\pi\sqrt{n_1^2 sin^2\theta_i - n_2^2}} \tag{1}$$

where λ_0 is the wavelength of the light launched into the fibers, θ_i is the incidence angle of the light rays at the interface between the fiber core and medium, n_1 and n_2 are the RI of the optical fiber core and the RI of the surrounding medium, respectively. In order to increase the interaction of the evanescent field with the external medium for RI sensing of the optical fiber, the safe plastic jacket and the cladding of the optical fiber of sensing region must be removed, as shown in Fig. 1. When a part of the FBG cladding is removed along the grating region such that the core modes interact with the surrounding environment, the values of effective refractive index of the waveguide modes are directly affected by the external medium refractive index, leading to a shift in the reflected wavelength (λ_B), given by [21]:

$$\partial\lambda_B = 2\Lambda\eta_{p0}\left(n_2 - n_3\right), \tag{2}$$

where The Bragg grating wavelength (λ_B) is the center wavelength of the light reflected from a Bragg grating, n_3 is the RI of the optical fiber cladding, Λ is the periodicity of the Bragg grating, and η_{P0} is the fraction of the total power of the unperturbed fundamental modes that flow in the removed region and therefore lost to the external medium. In this experiment, the prepared D-shape FBG is fabricated via the side-polishing technique. The cladding of the original FBG section is side-polished to form the D-shaped FBG sensing probe. The schematic diagram of side-polishing technique is shown in Fig. 2(a). The prepared D-shaped FBG is performed by stripping over a section of the safe plastic jacket of the original FBG and then the cladding of the original FBG is side-polished following two steps. In the first step (rough polishing), a polishing wheel coated with 50 µm diamond particle to coarsely grind the cladding of the original FBG with large surface roughness. Then, the second step (fine polishing) is performed by using a polishing wheel coated with 0 8 µm diamond particle to finely polish the D-shaped FBG surface to reduce surface roughness and avoid scattering of light. Finally, the polished surface of D-shaped FBG is carefully cleaned in ethanol solution using ultrasound. During the polishing process, the broadband light source from amplified spontaneous emission (ASE) of Erbium-doped fiber amplifier (EDFA) and the optical spectrum analyzer (OSA) with high resolution of 0.01 nm (Advantest Q8384) are used to monitor the quality of the polishing process via the transmission spectrum of Bragg resonant D-shaped FBG.

II.2. Build of loop-mirror optical fiber laser

The proposed refractometer is build based on the D-shaped FBG integrated in a loop-mirror optical fiber laser, as shown in Fig. 2(b).

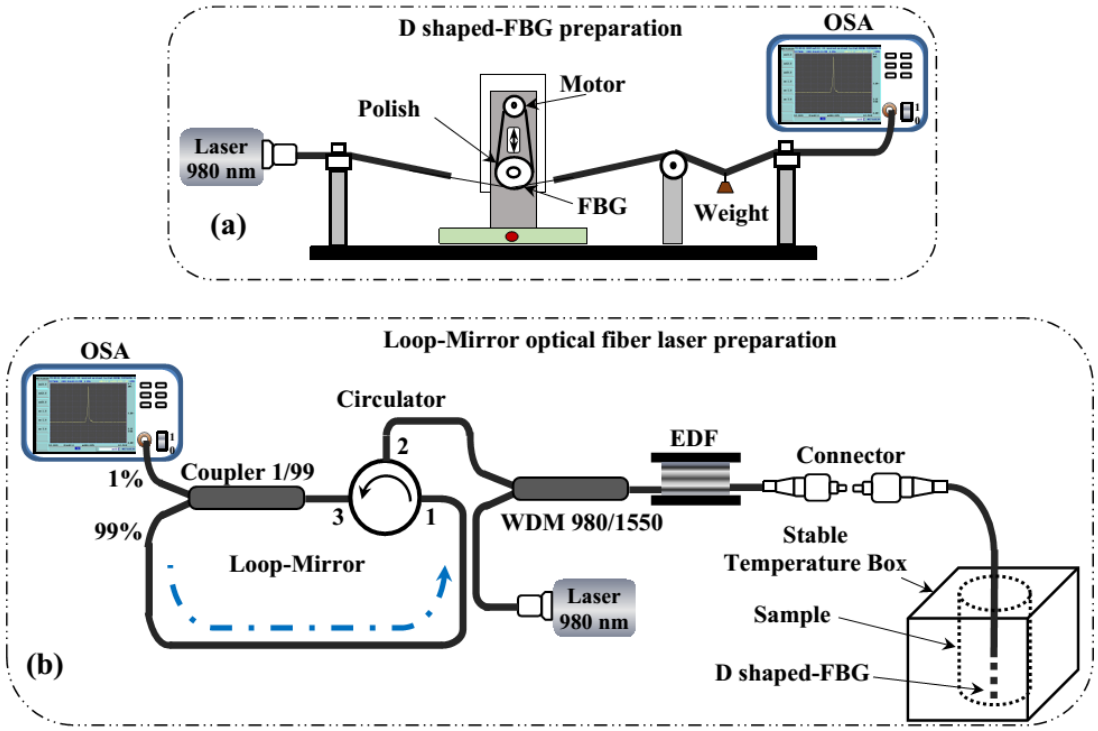

Fig. 2. Schematic diagram of D shaped-FBG polishing (a) and loop mirror optical fiber laser (b).

The gain medium is a 3.5 m long erbium doped fiber (Model: EDF-HCO-4000, Coractive, CANADA) which is pumped by a laser diode at 980 nm with output optical power up to 182 mW in single-mode emission (SDLO-2568-200). The erbium ions are then excited by connecting this laser diode to a 980/1550 nm wavelength division multiplexer (WDM. The other end of the erbium doped fiber is connected to the D-shaped FBG sensing element acting as a mirror of the fiber laser system. A fiber-optic circulator is used to couple the light into the cavity via an optical coupler 1/99. This set-up allows 1% of light leak from the cavity to the acquisition system while 99% of light return to the cavity. Therefore, a narrow line-width of lasing emission with high optical signal-to-noise ratio can be generated. The loop mirror optical fiber laser is activated by the saturated pump technique. This technique helps optimize the output optical power (at 182 mW) of a 980 nm-laser diode so shat the saturated lasing response can be acquired. Therefore, the lasing spectrum signal is obtained at its maximum intensity. All the lasing spectral response is written by the OSA.

II.3. Preparation of sample and RI measurement

In our work, the measured samples are prepared by mixed solutions of glycerol and water in order to provide different RI solutions. The proposed refractometer using a D-shaped FBG integrated in a loop-mirror optical fiber laser is performed for measuring its reflection spectra and lasing intensity in different RI solutions following a measurement setup as depicted in Fig. 2(b). During the measuring process, the prepared D-shaped FBG is dipped into the prepared different RI solutions in which all the measuring samples are maintained at a stable temperature inside a stable temperature box at room temperature of 25˚C. After each measuring time, the D-shaped FBG sensing probe is taken out from the measuring samples and carefully cleaned in the de-ionized water using ultrasound to completely remove any residual measuring sample. All achieved sensing spectral responses are written by OSA with high resolution of 0.01 nm (Advantest Q8384).

III. RESULTS AND DISCUSSION

III.1. Morphological features of D-shaped FBG sensing probe

The polished surface of the obtained D-shaped FBG can be observed by its Scanning Electron Microscopy (SEM) images, as presented in Fig. 3.

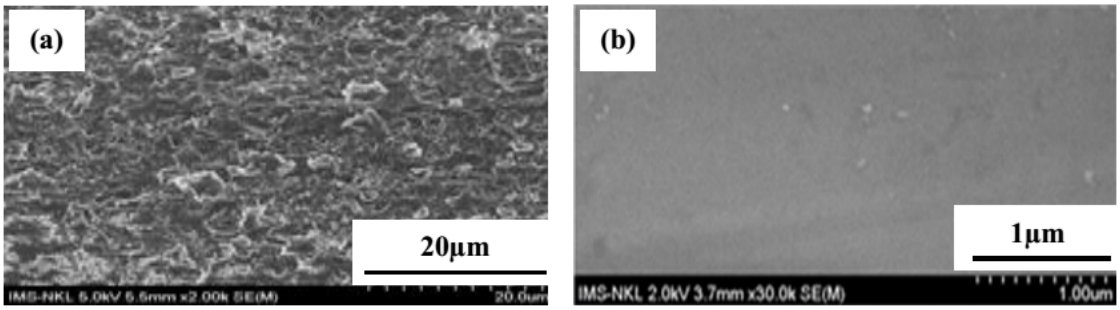

Fig. 3. SEM images of D shaped-FBG surface after side-polishing in the first step processing (a) and the second step processing (b).

Figure 3(a) shows SEM image of the D-shaped FBG surface after performing side-polishing technique in the first step processing (rough polishing). It is observed that the D-shaped FBG surface roughness is very large and thus would result in the decrease in the intensity of the sensing spectral response due to the scattering of light. Fig. 3(b) depicts SEM image of the final D-shaped FBG surface after the second step processing (fine polishing). As the final D-shaped FBG surface now becomes smooth, the D-shaped FBG sensing probe enhances the sensing signal due to the reduction of scattering of light.

III.2. Characteristics of sensing signals

The experimental results of investigating the sensing signal characteristics of the D-shaped FBG integrated in the loop-mirror optical fiber laser employed the same D-shaped FBG sensing probe obtained for different RI solutions is shown in Fig. 4.

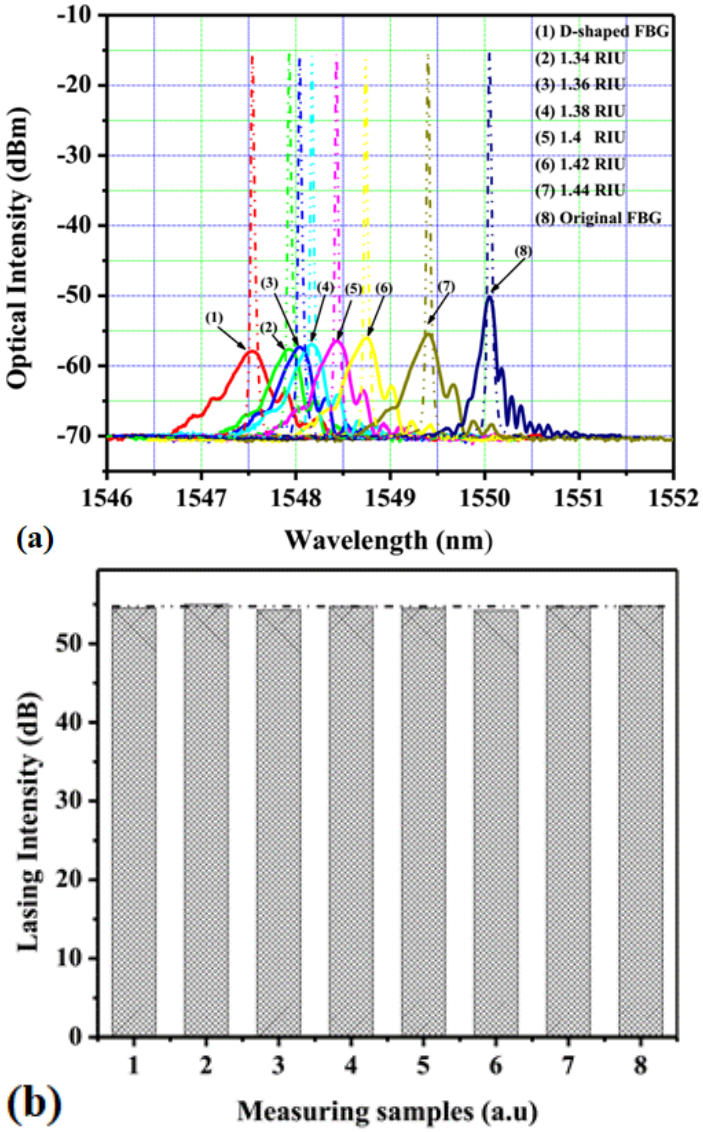

Fig. 4. The reflection spectra (solid lines) and lasing spectral response (dash dot dot lines) (a), and lasing intensity (b) of sensing signals in different RI solutions.

Figure 4(a) depicts the reflection spectra (solid lines) and lasing spectral response (dash dot dot lines) of the sensor. The sensing spectral response of the fabricated D-shaped FBG with Bragg resonant wavelength of 1547.54 nm, linewidth of 0.62 nm is depictured in Fig. 4(a) at sample (1) while the sensing spectral response of the original FBG sensing probe with Bragg resonant wavelength of 1550.05 nm, linewidth of 0.22 nm and reflectivity of 67% is shown in Fig. 4(a) at sample (8). The original FBG area is side-polished to close up the central FBG core, the FBG resonance wavelength shift is of 2.51 nm. The obtained D-shaped FBG is ready to employ as the

sensing probe for determination of RI of different solutions. The sensing spectral responses using the D-shaped FBG in different RI solutions in the range of 1.34 – 1.44 are also shown from sample (2) to sample (7), respectively. A non-linear redshift is occurred in spectral response of the sensor when the RI of the solutions increases in this range of RI, because the polished FBG of the Bragg grating wavelength creates a blue shift from 1550.05 nm (as shown in Fig. 4(a) at sample 8) to 1547.54 nm (as shown in Fig. 4(a) at sample 1) due to the fact that the core modes interact with the surrounding environment by the optical mode to penetrate evanescently into the surrounding environment. Therefore, when the RI of the surrounding environment increases closed to the RI of the FBG cladding (i.e., 1.445), a non-linear red shift occurred in the case using the polished FBG of the Bragg grating wavelength (as shown in Fig. 4(a) at sample 2 to 7), as elucidated by Eq. (2). It is also noticed that there is quite big difference in the intensity of these two spectra. The intensity of the reflection spectra is very low at about -55.15 dBm while the linewidth of the reflection spectra (full width at half-maximum: FWHM) is large at about 0.62 nm. The wavelength of the reflection spectra runs to longer wavelength range, but at the same time the intensity of the reflection spectra also increases for larger RI of the solutions. Because the optical mode penetrates evanescently into the surrounding environment and the total power of the fundamental waveguide modes thus attenuates to the surrounding environment, when the RI of the surrounding environment increase closed to the RI of the FBG cladding (i.e., 1.445) this penetration is decreased, following to Eq. (1). The lasing spectral response of the sensor with the D-shaped FBG integrated in the loop-mirror optical fiber laser is very strong at about -16.38 dBm, much higher than the intensity of the reflection spectra and the FWHM is much narrower at about 0.01 nm. The saturated pump technique is applied to the loop-mirror optical fiber laser integrated D-shaped FBG by a 980 nm-laser diode with the output optical pump power of 182 mW, hence the lasing spectral response achieve at the maximum intensity and stable as the RI of solutions change, as shown in Fig. 4(b). The LOD is defined based on the sensitivity S and the Q-factor of $\lambda/\delta\lambda$, in which $\delta\lambda$ is the linewidth of spectrum [32]:

$$LOD = \frac{\lambda}{Q * S} \tag{3}$$

In this study, we have proposed a optical fiber refractometer using a loop-mirror optical fiber laser structure integrated a D-shaped FBG. With obtained experiment results have shown that the linewidth of the sensing spectral response is very narrow about 0.01 nm, compare to D-shaped FBG sensor using the measured reflection configuration with the linewidth of the sensing spectral response about 0.62 nm. Following to Eq. (3):

$$LOD = \frac{\lambda}{Q * S}(3) \Rightarrow \frac{LOD_{LD}}{LOD_{Ref}} = \frac{Q_{Ref}}{Q_{LD}} = \frac{\delta\lambda_{LD}}{\delta\lambda_{Ref}} \approx 0.016$$

Therefore, the characteristics of the lasing spectral response of the sensor has been improved then the detection accuracy and the LOD of the sensor based on the D-shaped FBG integrated in the loop-mirror optical fiber laser are enhanced.

III.3. Results of RI measurements

In our experiments, the feasibility of the proposed refractometer is proven by carrying out the measurement with variable RI in the range of 1.42-1.44, as shown in Fig. 5.

It is perceived that the lasing wavelength clearly shifts towards longer wavelength as the RI of solutions increases in the range of 1.42-1.44. With the saturated pump technique, the lasing intensities are very strong and stable as the RI of solutions increases in the range of 1.42-1.44.

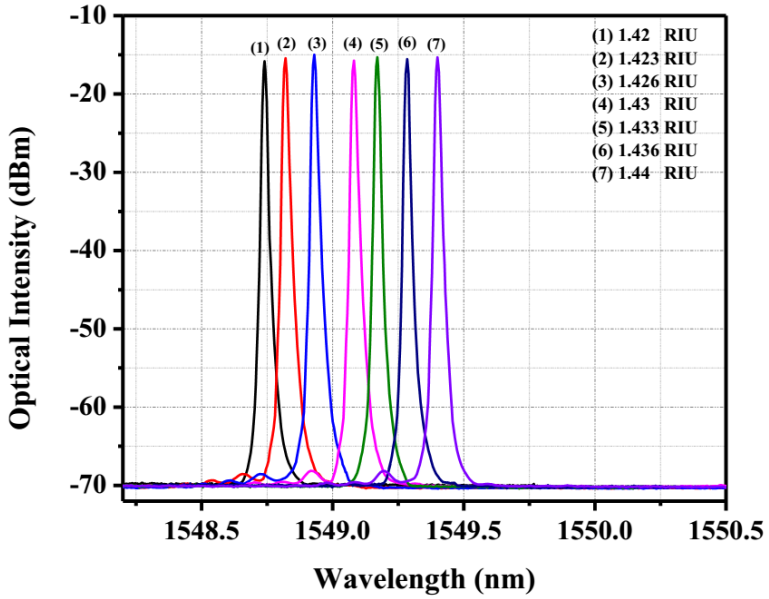

Fig. 5. The lasing spectral response of the proposed refractometer in solutions with variable refractive index in the range of 1.42-1.44.

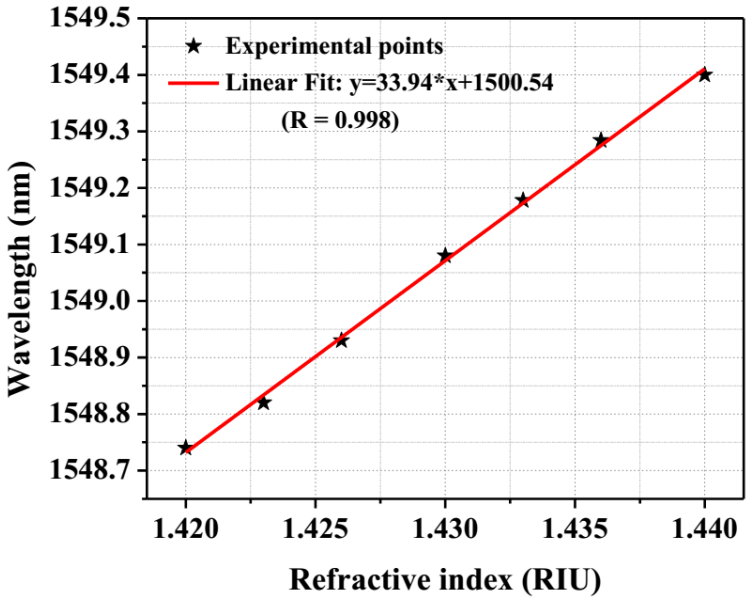

Fig. 6. Linear fitting relationship between Bragg wavelength and refractive index.

Fig. 6 represents the dependence of the wavelength of lasing spectral response of the sensor on the refractive index in the range of 1.42 to 1.44 and the achieved sensitivity is 33.94 nm/RIU. The linear fitting method is used to fit the experimental results and a good linearity has been obtained, given as $y = 33.94 * x + 1500.54$ with r square of 0.998. The LOD is estimated as 2.95×10^{-4} RIU, which has been greatly improved in comparison with the reflection or the transmission spectra of sensor [27]. Because of the narrow linewidth of lasing spectral response of the sensor of about 0.01 nm, the Q factor of sensor is thus very high. This achieved result of the sensor shows that the proposed sensor may be useful in bio-chemical sensing.

IV. CONCLUSIONS

In summary, we successfully propose and prepare a novel RI sensor with a D-shaped FBG sensing integrated into a loop-mirror optical fiber laser. The sensing characteristics of the proposed sensor have been improved and the intensity of the sensing spectral response is very strong and stable of about -16.38 dBm while the very narrow linewidth of about 0.01 nm via the using the saturated pump technique is achieved. The experimental results also demonstrate the feasibility of this sensor in measuring refractive index range from 1.42 to 1.44 RIU with high sensitivity of 33.94 nm/RIU and LOD of 2.95×10^{-4} RIU. This kind of RI sensor will serve broad applications in biochemical sensing due to its simple structure and stable performance.

ACKNOWLEDGMENT

This work is financially supported by the National Foundation for Science and Technology Development of Vietnam (NAFOSTED) under grant No. 103.03-2018.306.

REFERENCES

[1] S. Sounderajan, A. C. Udas, and B. Venkataramani, *Characterization of arsenic (V) and arsenic (III) in water samples using ammonium molybdate and estimation by graphite furnace atomic absorption spectroscopy*, *J. Hazard. Mater.* **149** (2007) 238.

[2] N. Zhang, N. Fu, Z. T. Fang, Y. H. Feng and L. Ke, *Simultaneous multi-channel hydride generation atomic fluorescence spectrometry determination of arsenic, bismuth, tellurium and selenium in tea leaves*, *Food Chem.* **124** (2011) 1185.

[3] S. Galani-Nikolakaki, N. Kallithrakas-Kontos and A. A. Katsanos, *Trace element analysis of Cretan wines and wine products*, *Sci. Total Environ.* **285** (2002) 155.

[4] L. J. Santos and M. T. Galceran, *The application of gas chromatography to environmental analysis*, *TrAC Trend. Anal. Chem.* **21** (2002) 672.

[5] H. Wei, S. M. H. Abtahi and J. Vikesland, *Plasmonic colorimetric and SERS sensors for environmental analysis*, *Environ. Sci.: Nano* **2** (2015) 120.

[6] M. Li, S. K. Cushing and N. Q. Wu, *Plasmon-enhanced optical sensors: a review*, *Analyst* **140** (2015) 386.

[7] T. T. Cao, H. B. Nguyen, V. T. Nguyen, T. T. Vu, M. Bayle, M. Paillet, J. L. Sauvajol, B. T. Phan, D. L. Tran, N. M. Phan and V. C. Nguyen, An interdigitated ISFET-type sensor based on LPCVD grown graphene for ultrasensitive detection of carbaryl *Sens. Actuators B Chem.* **260** (2018) 78.

[8] A. V. Markin, N. E. Markina and I. Y. Goryalcheva, *Raman spectroscopy based analysis inside photonic-crystal fibers*, *TrAC Trend. Anal. Chem.* **88** (2017) 185.

[9] Y. Chen, Q. Xie, X. Li, H. Zhou, X. Hong, Y. Geng, *Experimental realization of D-shaped photonic crystal fiber SPR sensor*, *J. Phys. D: Appl. Phys.* **50** (2017) 025101.

[10] T. B. Pham, H. Bui, H. T. Le and V. H. Pham, *Synthesis and deposition of Silver nanostructures on the silica microsphere by laser-assisted photochemical method for SERS applications*, *Sensors* **17** (2017) 0007.

[11] X. Wang and O. S. Wolfbeis, *Fiber-optic chemical sensors and biosensors (2013–2015)*, *Anal. Chem.* **88** (2016) 203.

[12] B. N. Shivananju, S. Yamdagni, R. Fazuldeen, A. K. Sarin Kumar, G. M. Hegde, M. M. Varma and S. Asokan, *CO_2 sensing at room temperature using carbon nanotubes coated core fiber Bragg grating*, *Rev. Sci. Instrum.* **84** (2013) 065002.

[13] N. Cennamo, D. Massarotti, L. Conte and L. Zeni, *Low cost sensors based on SPR in a plastic optical fiber for biosensor implementation*, *Sensors* **11** (2011) 11752.

[14] X. D. Wang and O. S. Wolfbeis, *Fiber-optic chemical sensors and biosensors (2015–2019)*, *Anal. Chem.* **92** (2020) 397.

[15] D. L. Presti, C. Massaroni, C. S. J. Leitao, M. D. F. Domingues, M. Sypabekova, D. Barrera, I. Floris, L. Massari, C. M. Oddo, S. Sales, I. I. Iordachita, D. Tosi and E. Schena, *Fiber Bragg Gratings for Medical Applications and Future Challenges: A Review*, *IEEE Access* **8** (2020) 156863.

[16] R. Zhang, S. Pu and X. Li, *Gold-film-thickness dependent SPR refractive index and temperature sensing with hetero-core optical fiber structure*, *Sensors* **19** (2019) 4345.

[17] N. Cennamo, L. Zeni, F. Arcadio, E. Catalano and A. Minardo, *A novel approach to realizing low-cost plasmonic optical fiber sensors: light-diffusing fibers covered by thin metal films*, *Fibers* **7** (2019) 34.

[18] Y. Tan, Z. Tou, K. Chow and C. Chan, *Graphene-deposited photonic crystal fibers for continuous refractive index sensing applications*, *Opt. Express* **23** (2015) 31286.

[19] R. Tan, S. Yap, S. Tjin, M. Ibsen, K. Yong and W. Lai, *Functionalized fiber end superstructure fiber Bragg grating refractive index sensor for heavy metal ion detection*, *Sensors* **18** (2018) 1821.

[20] W. Hu, C. Li, S. Cheng, F. Mumtaz, C. Du and M. Yang, *Etched multicore fiber Bragg gratings for refractive index sensing with temperature in-line compensation*, *OSA Continuum* **3** (2020) 1058.

[21] H. Bui, T. B. Pham, V. A. Nguyen, V. D. Pham, T. C. Do, T. V. Nguyen, T. H. C. Hoang, H. T. Le and V. H. Pham, *Novel method of dual fiber Bragg gratings integrated in fiber ring laser for biochemical sensors*, *Meas. Sci. Technol.* **29** (2018) 055105.

[22] A. K. Paul, *Design and analysis of photonic crystal fiber plasmonic refractive Index sensor for condition monitoring of transformer oil*, *OSA Continuum* **3** (2020) 2253.

[23] T. Schuster, R. Herschel, N. Neumann and C. G. Schaffer, *Miniaturized long-period fiber grating assisted surface plasmon resonance sensor*, *J. Lightwave Technol.* **30** (2012)1003.

[24] T. Wang, K. Liu, J. Jiang, M. Xue, P. Chang and T. Liu, *Temperature-insensitive refractive index sensor based on tilted moiré FBG with high resolution*, *Opt. Express* **25** (2017) 14900.

[25] Z. W. Ding, T. T. Lang, Y. Wang and C. L. Zhao, *Surface plasmon resonance refractive index sensor based on tapered coreless optical fiber structure*, *J. Lightwave Technol.* **35** (2017) 4734.

[26] Z. Liu, Y. Wei, Y. Zhang, E. Zhao, J. Yang and L. Yuan, *Twin-core fiber SPR sensor Opt. Lett.* **40** (2015) 2826.

[27] R. X. Tan, D. Ho, C. H. Tse, Y. C. Tan, S. W. Yoo, S. C. Tjin and M. Ibsen, *Birefringent Bragg grating in C-shaped optical fiber as a temperature-insensitive refractometer*, *Sensors* **18** (2018) 3285.

[28] A. Patnaik, K. Senthilanathan and R. Jha, *Graphene-based conducting metal oxide coated d-shaped optical fiber SPR sensor*, *IEEE Photon-Technol. Lett.* **27** (2015) 2437.

[29] C. Liao, Q. Wang, L. Xu, S. He, J. Zhao, Z. Li and Y. Wang, *D-shaped fiber grating refractive index sensor induced by an ultrashort pulse laser*, *Appl. Opt.* **55** (2016) 1525.

[30] F. Sequeira, D. Duarte, L. Bilro, A. Rudnitskaya, M. Pesavento, L. Zeni and N. Cennamo, *Refractive index sensing with d-shaped plastic optical fibers for chemical and biochemical applications*, *Sensors* **16** (2016) 2119.

[31] L. Jiao, N. Zhong, X. Zhao, S. Ma, X. Fu and D. Dong, *Recent advances in fiber-optic evanescent wave sensors for monitoring organic and inorganic pollutants in water*, *TrAC Trend. Anal. Chem.* **127** (2020) 115892.

[32] W. Xu, J. Flueckiger, S. Schmidt, S. Grist, S. T. Fard, J. Kirk, M. Doerfler, K. C. Cheung, D. M. Ratner and L. Chrostowski, *A silicon photonic biosensor using phase-shifted Bragg gratings in slot waveguide*, *J. Biophotonics* **6** (2013) 821.